Article

Satellite-Based Monitoring of Growing Agricultural Water Consumption in Hyper-Arid Regions

Ashkan Ebrahimivand [1], Farhad Hooshyaripor [1,*], Salar Rezaei-Gharehaghaj [1], Sahand Razi [1], Mohammad Milad Salamttalab [2], Mahdi Kolahi [3] and Roohollah Noori [4,5,*]

[1] Faculty of Civil Engineering, Science and Research Branch, Islamic Azad University, Tehran 1477893855, Iran
[2] School of Civil Engineering, Iran University of Science and Technology, Tehran 1684613114, Iran
[3] Department of Rangeland And Watershed Management, Faculty of Natural Resources and Environment, Ferdowsi University of Mashhad, Mashhad 9177948974, Iran
[4] Graduate Faculty of Environment, University of Tehran, Tehran 1417853111, Iran
[5] Faculty of Governance, University of Tehran, Tehran 1439814151, Iran
* Correspondence: hooshyarypor@srbiau.ac.ir (F.H.); noor@ut.ac.ir (R.N.)

Abstract: Land-use change has a key role in hydrologic processes and biodiversity. Although many satellite-based studies have been conducted to reveal the interaction between land-use changes in hydrological processes worldwide, the land-use change impact on agricultural water consumption in hyper-arid regions is poorly understood. Here, we investigate increased agricultural water consumption in the Qom province, a hyper-arid region in Iran, using derived imageries from Landsat 5 Tm and Landsat 8 OLI during the last three decades. We used maximum likelihood classification (MLC) and decision tree classification (DTC) to analyze the satellite images. The MLC method showed that croplands have increased from 30,547 ha in 1989 to 39,255 ha in 2019 (i.e., a 29% increase). In this period, the total orchard area increased from 3904 ha to 6307 ha, revealing a growth of 61%. In the DTC method, the increases in the cropland and orchard areas were, respectively, 34% and 60%. Although both MLC and DTC satisfied the accuracy criteria, the former was more consistent than the latter concerning ground data and documented statistics. Satellite-based and MLC results showed an increase in agricultural water consumption from 152 million cubic meters (MCM) in 1989 to 209 MCM in 2019, showing a 38% increase (i.e., 1.27% annually). Our findings send an alarming message for policymakers to reduce the water demand through sustainable agricultural practices in the Qom province, where the agricultural sector uses approximately 90% of annual water demand.

Keywords: clustering; decision tree; land use; maximum likelihood; remote sensing; water consumption

1. Introduction

The amount of change in land use and land cover due to human activities or natural factors can be assessed using present or archived remote sensing data [1]. Land-use change can affect land cover, biodiversity, and aquatic ecosystems. Therefore, these changes in watersheds can affect water quality and can increase surface runoff as well as groundwater consumption. Land-use change information is important for water resource management so that it can show the effects of land-use changes on water-demand quality and quantity [2,3]. Ground-based studies using remote sensing techniques are a vital tool for generating rational information for making scientific decisions in natural resource management. In the tropics, it has been proven that human activities are the main cause of change in the land used. Humans are the cause of direct or indirect pressures on land and a constant threat to natural resources. Human intervention harms the livelihood of those in need of these lands [4]. Various processes that can be said to contribute to global environmental problems include pollution, global warming, ozone depletion, acid rain, depletion of natural resources, overpopulation, waste disposal, deforestation, and loss of biodiversity.

Almost all these processes are the result of the use of natural resources in an unsustainable manner [5]. Land protection is one of the issues that should be noticed by governments. It seems that, at the current level of human knowledge and technology, achieving a huge database in the above field without spending exorbitant costs will be possible using the science and technology of remote sensing. Remote sensing puts us well beyond the limits of human ability and provides information concerning areas that humans can not directly identify because of their dangerousness, high cost, and distance.

Today, many researchers in different countries use satellite information and remote sensing to monitor changes in forests, rangeland, and land use and to study the cultivated area, surface water, and river network [6,7]. To detect the reasons for variations over a 20-year period, Hussain et al. [8] identified the land-use and land-cover (LULC) changes in the Okara district over 3 years (2000, 2010, and 2020). They used various Landsat images and supervised classification in their study. Lagrosa et al. [9] created a LULC classification scheme by incorporating ecological data to redefine classes based on variation in above-ground tree carbon. Zarandian et al. [10] investigated the effects of land cover changes and vegetation loss under the condition of change in the climatic parameters (temperature and precipitation) to determine the impacts on different ecological functions in the eastern Lake Urmia Basin in northwestern Iran. Liang et al. [11] investigated the Minjiang River Basin, where the forest area accounts for 65.42% of the total basin. Using MLC-supervised classification, they distinguished forest, cultivated land, unused land, construction land, garden land, and the water body of the basin. Regarding the significance of water resources, Saraf and Vejahat [12] scrutinized the potential of surface waters and their hydraulic and hydrological conditions in the Namak Lake watershed and the results showed that the study area has very good water resources compared to neighboring basins and basins with the same conditions. Chughtai et al. [13] collected the traditional pre and post-classification change detection techniques related to LULC information at the regional level. They evaluated the most-used change detection method and concluded the post-classification change detection method using the maximum likelihood classifier is applicable in all cases. Rohani et al. [14] compared the trend of climatic parameters and the water zones of Qom province changes using graphical representation and appropriate statistical tests and images of Landsat satellites to determine the similarity between these trends. Verma et al. [15] determined the long-term effects of land-use/land-cover change on surface water and groundwater resources of quaternary aquifers in the Lucknow area of the Ganga Plain based on a multi-temporal analysis of satellite and field data. Changes in land use and land cover for 2008 and 2016 were determined using Landsat 7 and Landsat 8 satellite data using classification techniques. The results showed a 4.09% increase in constructed land, a 5.49% increase in open land, an 8.8% decrease in vegetation, a 2.31% decrease in agricultural land, and a 3.35% decrease in surface water level. Hu et al. [16] examined land-use change and land cover in Guangxi, China. They used satellite image processing and used Markov chain analysis and change matrices between 1990 and 2017 to determine the likelihood that each user category would change to another. They analyzed the deforestation process during this period. According to the results of this research, the total amount of changes in this area was 4708 km^2, of which 418 km^2 were related to deforestation.

Qom is one of Iran's provinces located on the central plateau of Iran. Most of its area is in the arid and desert regions. The seasonal Qomroud and Qarachai rivers flow through this province and finally discharge into Namak Lake [17]. Although there are limited water resources in the province, the development of agricultural lands in the region has increased rapidly over the last three decades. As a result, several water transfer projects have been designed and implemented to provide water from adjacent basins, apparently to provide drinking water. Although some studies have been conducted on land-use changes in the Qom province [18], no specific study has been conducted to investigate the increase in water demand in this important province. This paper attempts to show the trend of agricultural land growth in an arid area with water resource limitations. In addition,

a comparison is made here between maximum likelihood classification (MLC) and decision tree classification (DTC) to evaluate the importance of the classification method in satellite image analysis.

2. Study Area

Iran is divided into six main catchments [19], and the Central Plateau, with an area of approximately 825,000 km^2, consists of 51% of the total area of Iran. According to the precipitation, this basin can be divided into three parts: semiarid, arid, and very arid, with an average annual rainfall of 330, 125, and 75 mm [19,20]. The average long-term rainfall in the Central Plateau is approximately 155 mm/yr, while the minimum value was recorded in 2008 with 45 mm/yr of precipitation. This region experienced a more than 30% decrease in rainfall in 2013 and 2015. On the other hand, water demand has increased in this region because of the rapid increase in the population, health and welfare improvement, development of the economic sectors, and immigration to the city of Qom. Qom province, with an area of 11,240 km^2, is located near the central desert of Iran and in the neighborhood of Iran's capital. The province is located between 50°15′ and 52° east longitude and 34°10′ and 35°10′ north latitude (Figure 1). According to statistics and information, the average annual rainfall in Qom province is 135 mm. The population of Qom province in 1996 was 777,677, which increased to 1,201,158 in 2016, with a growth rate of 2.7% per year. The population density of Qom province is 112 people per square kilometer, which is the fifth most densely populated province in Iran [21]. As mentioned, most of Qom province is in the arid and desert region, and two rivers, Qamroud and Qarachai, flow from the watershed up to discharge to Namak Lake [17]. The amount of water entering these rivers to the province before the construction of the 15 Khordad and Ghadir Saveh dams was equal to 698 million cubic meters (mcm). In addition, the surface water from rainfall was estimated at 50 mcm. Consequently, the total volume of surface water in the province reached 750 mcm. The volume of output water from this basin, at the site of Kuh-e Sefid station, was 261 mcm before the mentioned dams, while after the construction of the two dams, it was reduced to 66 mcm. With the construction of these two dams, the inflow of water by the Qamroud and Qarachai rivers to Qom province was reduced. The volume of renewable groundwater in the province is estimated at 694 mcm.
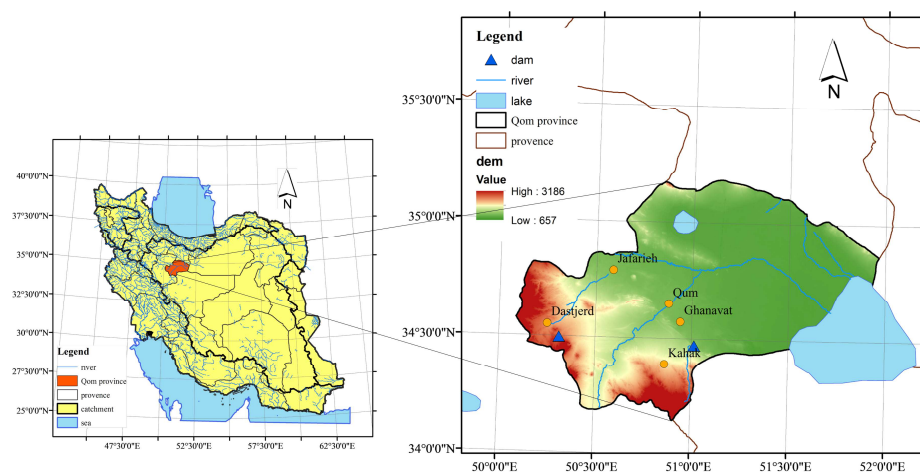
Figure 1. Location of Qom province in Iran.

3. Materials and Methods

In this paper, the remote sensing technique was used to study the trend of land-use change. The study includes a 30-year period between 1989 and 2019. For this reason, 10 images from two main sensors, Landsat 5 Thematic Mapper (TM) and Landsat 8 Operational Land Imager (OLI) (U.S. Geological Survey, Reston, VA, USA), were used in different years: 1989, 1999, 2008, 2014, and 2019. Landsat 5 TM images consist of seven spectral bands with a spatial resolution of 30 m for Bands 1 to 5 and 7. The spatial resolution for

Band 6 (thermal infrared) is 120 m but is resampled to 30 m pixels. The other Landsat 8 OLI and Thermal Infrared Sensor (TIRS) images consist of nine spectral bands with a spatial resolution of 30 m for Bands 1 to 7 and 9. The resolution for Band 8 (panchromatic) is 15 m. Thermal bands 10 and 11 are useful in providing more accurate surface temperatures and are collected at 100 m. The images were acquired in the spring and autumn of each year. The images were obtained from the United States Geological Survey website (https://earthexplorer.usgs.gov/; accessed on 12 May 2021). Then, pre-processing, processing, and post-processing of satellite images were applied to obtain land-use maps.

3.1. Image Pre-Processing

The pre-processing stage includes radiometric correction of images and mosaic techniques. Here, land-use change is tracked according to the numerical values of pixels over time. To be able to assess changes over a while, comparative images need to be as relevant as possible to similar times in different years. Radiometric correction in Landsat 8 and 5 images was performed by converting the digital numbers to brightness temperatures in thermal bands and converting a digital number to reflectance in reflective bands. Figure 2 shows the Qom province area in the mosaic image in 2019.
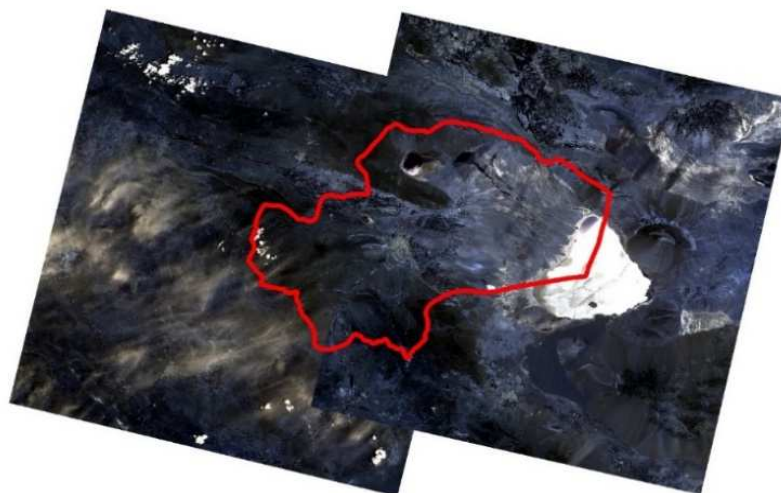
Figure 2. Qom province area in mosaic images (12 and 19 May 2019).

3.2. Image Processing

The first stage in any classification method is to define different required classes. To separate the land use classes in the best possible way, one must correctly identify the various features and phenomena of the earth's surface. Choosing the right band composition is important for separating the land uses better. Downloaded satellite images can provide different bands, such as NIR, RED, and SWIR, that can be received by different ranges of image processing software. These bands can be used in combination with each other or in the calculation of various indices, such as NDVI, to allow better recognition of different lands. Qom province is homogeneous in terms of land position and the shape of the phenomena; however, choosing the right band composition by itself is not helpful. Therefore, as well as multispectral compositions, indicators and topographic characteristics of the region are also used.

For delineating the agricultural areas and calculating the trend of changes in Qom province, two remote sensing approaches have been tested for classification: (1) thresholding methods (here, the DTC method) and (2) supervised/unsupervised pixel-based classification methods (here, the MLC method). In the case of the DTC method, in addition to the digital elevation model (DEM), the normalized difference vegetation index (NDVI) was used to classify vegetation classes and the normalized difference built-up index (NDBI)

was used for urban areas. The NDVI varies between -1 and 1, where positive values correspond to vegetation, and it can be calculated as follows [22].

$$NDVI = \frac{NIR - RED}{NIR + RED}, \tag{1}$$

where NIR is the near-infrared band (which is Landsat band 4 in TM and ETM meters and Landsat band 5 in OLI meters) and RED is the red band (which is Landsat band 3 in TM and ETM meters and Landsat band 4 in OLI meters).

NDBI is an index that can distinguish residential areas from other classes in dry areas without vegetation [23].

$$NDBI = \frac{SWIR - NIR}{SWIR + NIR}, \tag{2}$$

where SWIR is the short-wave infrared band.

The classes defined for the MLC are water body, bare land, urban area, rangeland, cropland, orchard, and others. For DTC, the classes are the same, but cropland was divided into two classes: spring and fall croplands.

3.2.1. Maximum Likelihood Classification

First, an equal number of samples are taken for each class because experience with machine learning methods has demonstrated that the number and quality of training samples are crucial factors in obtaining accurate results [24]; then, MLC is applied. MLC is a supervised classification method which is based on the Bayes theorem. It makes use of a discriminant function to assign a pixel to the class with the highest likelihood [25]. Among the supervised classification methods, MLC is one of the most efficient methods of image classification. In addition, the MLC method is a simple pixel-based method that is often used to detect land-use changes [18]. However, MLC is a good method for classification; however, sometimes, it is not able to classify mixed pixels correctly, which may lead to the loss of some information [19].

3.2.2. Decision Tree Classification

A decision tree is defined as a classification procedure that recursively partitions a data set into smaller subdivisions on the basis of a set of tests defined at each branch (or node) in the tree [26]. The focus of this study is on water consumption calculation. The emphasis of the research is on croplands and orchard classes. Vegetation and related indicators are used to increase the accuracy of the results in the DTC. Therefore, the NDVI index was used in this classification. The decision tree takes an object as input and then classifies it using a set of descriptions and simple equations.

3.3. Image Post-Processing

The accuracy of the classification indicates the level of trust in the extracted map. No classification method is complete until its accuracy has been assessed [25]. The results of the classification were assessed using the error matrix. An error matrix compares classification results to the observations on the ground as a standard. The elements of the matrix are calculated based on a comparison between field data (here samples taken from Google Earth and ground data provided by the Static Center of Iran [27]) and classification results in the model. The overall accuracy (OA) is the average of the classification accuracy and shows the number of correctly classified pixels compared to the total number of known pixels [28]:

$$OA = \frac{\sum P_{ii}}{N}, \tag{3}$$

where N is the total number of pixels, and P_{ii} is the sum of the values in the main diagonal of the error matrix. OA looks at all classes equally and does not take into account the differences that exist between classes. On the contrary, the Kappa coefficient ($\hat{K}$) also takes non-diagonal elements into account [26]. The Kappa coefficient, introduced by Cohen [25],

essentially evaluates how well the classification performed as compared to just randomly assigning values. The Kappa statistical index was

$$\hat{K} = \frac{P_o - P_e}{1 - P_e},$$

(4)

where P_o is the accuracy of the observed agreement, and P_e is the estimate of the chance agreement.

Furthermore, producer's accuracy (PA) and user accuracy (UA) are also defined separately to evaluate the classification accuracy for each class. PA measures how well a certain area has been classified as follows:

$$PA = \frac{N_A}{N_{Ag}},$$

(5)

where N_A is the number of correct pixels classified as class A, and N_{Ag} is the number of class A pixels in ground reality. The UA is the probability that a certain class on the ground is in the same class on the classified image, and it is, therefore, a measure of the reliability of the map, which is calculated as follows:

$$UA = \frac{N_A}{N_{Ac}},$$

(6)

where N_{Ac} is the number of pixels of class A as a result of classification. Based on the above accuracy indices, commission error (C_e) and omission error (O_e) are defined. The C_e is equivalent to the probability of pixels classified in a class that does not belong to that class [28]:

$$C_e = 1 - UA.$$

(7)

The O_e is equivalent to the percentage of pixels of a class that are classified as other classes [28]:

$$O_e = 1 - PA.$$

(8)

3.4. Estimation of Net Water Consumption

One of the important goals of this research is to obtain the amount of net water used in agricultural products. The field crops include grains, cereals, vegetables, melons, and fodder. Orchard products include seeded fruits, stone fruits, dried fruits, and subtropical fruits [29]. These products were used to calculate the average net water demand per hectare separately for croplands and orchards in the province. These values can be used for the estimation of total annual water consumption in the province as soon as the cropland and orchard areas are calculated by remote sensing every year. This simplification is considered because behind the high uncertainty, in this study, the cultivation pattern is not extracted in detail. Therefore, the average net water demand per hectare (AWD) can be obtained as follows:

$$AWD_j = \frac{\sum_{i=1}^{n} WC_i \, A_i}{\sum_{i=1}^{n} A_i} \forall j = 1 \ldots 2,$$

(9)

where A_i is the area of crop i, WC_i is the net water demand of crop i in Qom province, which can be obtained from the NETWAT crop water calculator [30], n is the number of crops, and j denotes the two separated agricultural sectors: cropland and orchards. Then, using the agricultural areas ($Area_j$) as the output of remote sensing analysis, the total net water consumption (TWC) of the agricultural sector can be calculated every year from Equation (10):

$$TWC = \sum_{j=1}^{2} \left(AWD_j . Area_j \right).$$

(10)

It should be emphasized that in this methodology, the water consumption of a crop over 30 years of the study is considered unchanged, although, because of technological

evolutions and the link between water consumption and agriculture strategies, the water consumption by a crop may vary from year to year [31].

4. Results and Discussion

4.1. Land Use over 30 Years

In MLC, at first, some samples of each class were taken, and then the classification method was applied. In the DTC, first, the data extracted from each layer of stacked images were classified, and then numerical constraints to each user were applied. Figures 3 and 4 show land-use maps based on MLC and DTC methods, respectively.
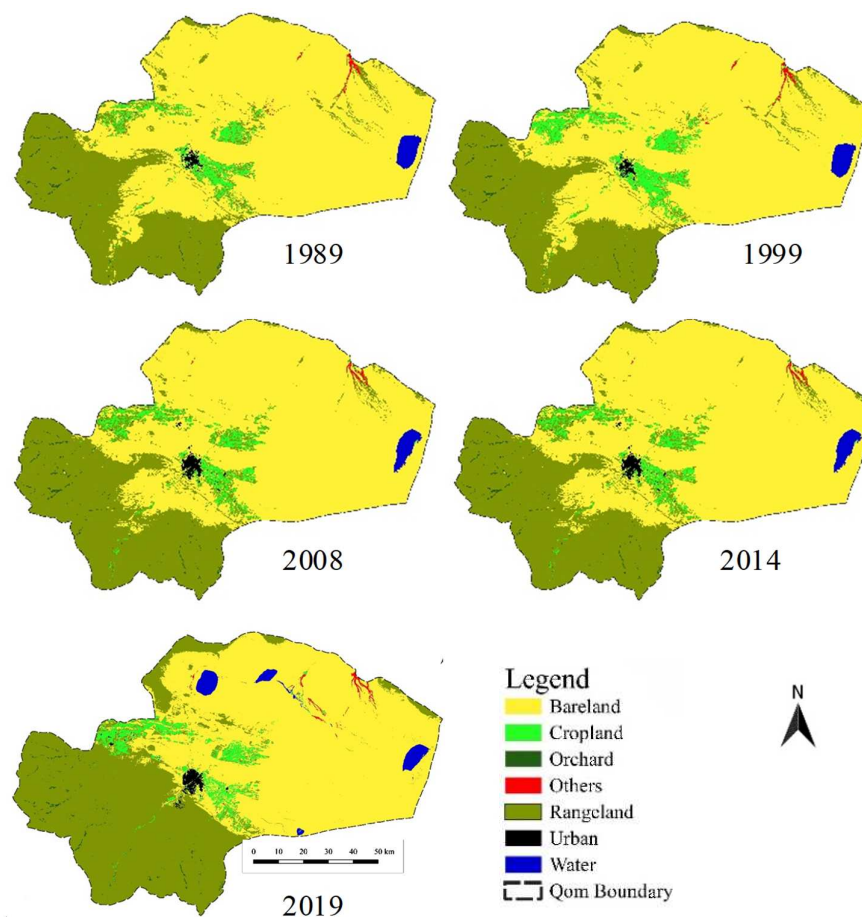
Figure 3. Qom land use in 1989, 1999, 2008, 2014, and 2019 using the maximum likelihood classification (MLC) method.

The overall accuracy and Kappa coefficient in MLC were 0.79 and 0.74, respectively. Furthermore, the results of overall accuracy and the Kappa coefficient in the DTC were 0.84 and 0.81, respectively. The other accuracy indices were calculated, and the results are presented in Table 1. According to [32], the level of acceptability for Kappa coefficients in the range of 0–0.2 is low. For coefficients between 0.21–0.4, it is moderate; between 0.41–0.6 is suitable, between 0.61–0.8 is acceptable, and for coefficients more than 0.81, it is excellent. Based on these ranges, the results of the MLC method are acceptable, and the results of the DTC method are excellent.
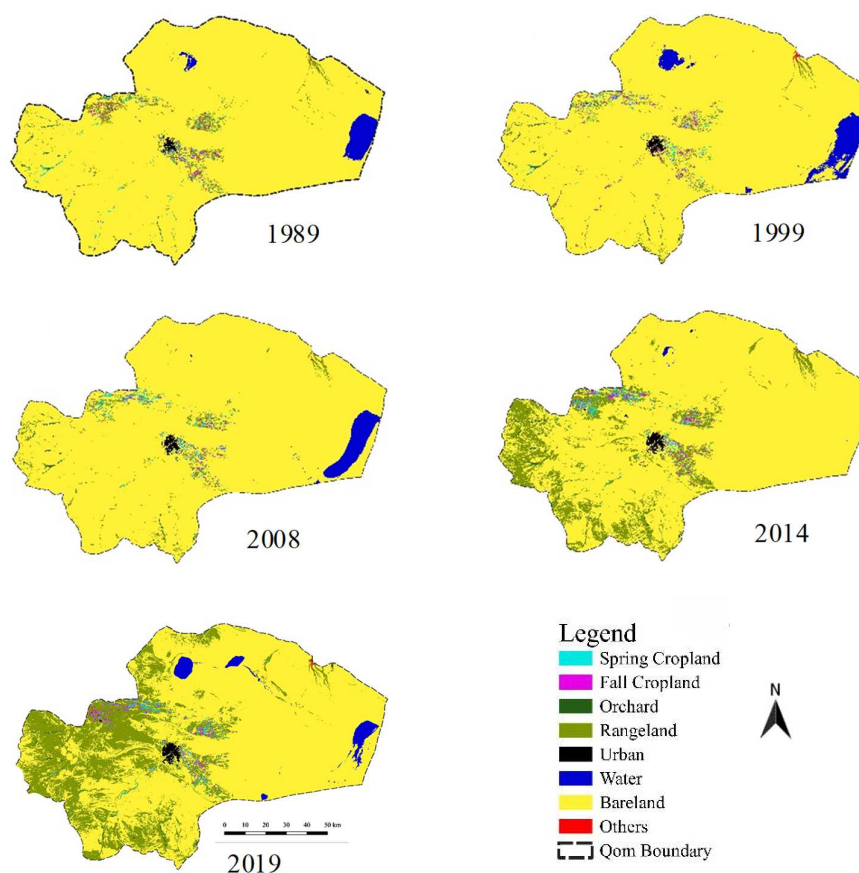
Figure 4. Qom land use in 1989, 1999, 2008, 2014, and 2019 using the decision tree classification (DTC) method.

Table 1. Values of error measures (%) for both MLC and DTC methods.

Index	Classification Method	Cropland	Orchard	Rangeland	Urban	Water	Bare Land
PA	DTC	83.33	86.84	83.33	71.88	89.47	96.15
	MLC	75	80.49	82.76	81.25	78.95	73.08
UA	DTC	89.74	100	75.76	100	100	52.52
	MLC	91.67	91.67	51.06	100	100	63.33
Oe	DTC	16.67	13.16	16.67	28.13	10.53	3.85
	MLC	25	19.51	17.24	18.75	21.05	26.92
Ce	DTC	10.26	0	24.24	0	0	40.87
	MLC	8.33	8.33	48.94	0	0	36.67

4.2. Trend of Land-Use Change

Once the accuracy of the classification maps has been examined, land-use change is examined. According to the results, the area of each class was calculated over the 30-year period. The description of the changes in each class for both classification methods is examined so that the amount of consumed water can be calculated. Tables 2 and 3 show the land-use areas of Qom province from 1989 to 2019 based on MLC and DTC methods. The obtained results show that the amount of rangeland area in 2019 compared to the entire 30-year period for both MLC and DTC has increased significantly. As the area of rangeland is directly related to the amount of rainfall (the higher the amount of rainfall, the greater the area of rangeland), it can be concluded that in 2019, the rainfall over the Qom province was more than the previous years. On the contrary, the bare land area decreased in 2019, which confirms this hydrologic condition. As can be seen, the largest area of land use in

both methods is bare land, which indicates the climatic conditions of Qom. In addition, the change in urban areas during these 30 years is significant. The urban area has increased as much as 44% and 51% for DTC and MLC methods, respectively. It is worth noting that the water body area has varied significantly in this period because of the existence of seasonal lakes, which deeply depend on the amount of precipitation in different years.

**Table 2.** Land-use area for the MLC method in hectares.

Land-Use \ Year	1989	1999	2008	2014	2019
cropland	30,546.81	34,340.85	34,039.8	39,108.33	39,255.03
orchard	3903.57	5286.69	5470.47	5745.6	6306.84
rangeland	335,022.7	306,292.1	356,932.5	319,030.5	446,187.5
urban	4309.74	4745.88	6030.36	6137.73	6547.86
water	9843.84	29,911.23	935.91	5709.33	17,401.77
bare land	765,847.08	770,640.2	738,251.9	775,568.8	632,671.8
others	2543.04	799.83	1931.67	716.31	4202.82

Table 3. Land-use area for the DTC method in hectares.

Land-Use \ Year	1989	1999	2008	2014	2019
spring cultivation	11,728.17	13,487.4	14,418.36	16,485.48	17,323
fall cultivation	11,880.81	11,022.03	7804.44	14,100.48	14,383.26
orchard	3571.47	3949.56	4172.22	4737.24	5754.24
rangeland	33,865.92	30,117.87	32,275.71	140,075.8	262,979.9
urban	4016.16	4167.63	4448.7	5127.39	5786.88
water	24,480.99	40,031.37	29,954.25	1209.69	22,538.52
bare land	1,062,503	1,048,405	1,058,963	970,571.5	823,176.9
others	523.8	1345.77	382.68	245.88	1227.15

　　　As water consumption is important in this study, the trend of agricultural land-use change is evaluated in the following ways. Figure 5 shows the trend of the changes in cropland and orchard classes for both MLC and DTC methods. According to Figure 5a, from 1989 to 2019, the area under cultivation of cropland has increased from 30,547 ha to 39,255 ha (regarding the MLC method), which shows a 28% growth (annually 0.93%). In the case of orchard areas (Figure 5b), MLC shows an increase of approximately 61% (from 3903 ha in 1989 to 6306 ha in 2019), which means 2.03% annually. However, regarding the DTC method, it was found that the area under cultivation of total croplands (spring and fall cultivation) increased from 23,609 ha to 31,706 ha, which shows 34% growth.

　　　According to the available data (Agricultural-Jihad Organization of Qom province, 2014), the cultivated area of croplands and orchards in 2014 were, respectively, approximately 42,300 ha and 8,700 ha. In comparison with the results of satellite image analysis for cropland areas (Tables 2 and 3), MLC has less error (7.5%) than DTC (15%). In the case of orchards, the MLC error is 34%, while DTC shows a 46% error in the results. This comparison proves that although both methods are reliable according to all accuracy indices (Table 1), the MLC method provides more accurate results compared to the recorded documents. It is worth mentioning that in the case of croplands, the error values are low, but for orchards, the errors are high. This may be because this research is related to two days of the year (one day in spring and one day in fall), so a limit of error may be accepted in this analysis. Although this attempt was made to use more satellite images, limitations such as distortion and cloud cover in the images made it impossible to use more accurate images. Additionally, the cultivated areas in the report of the Agricultural-Jihad Organization of Qom province [33] are calculated according to the agricultural products in a year, not by a field survey of lands. In such a condition, the area under cultivation may be overestimated due to higher products or vice versa. Therefore, it is not far from reality to have a difference between satellite results and statistics.
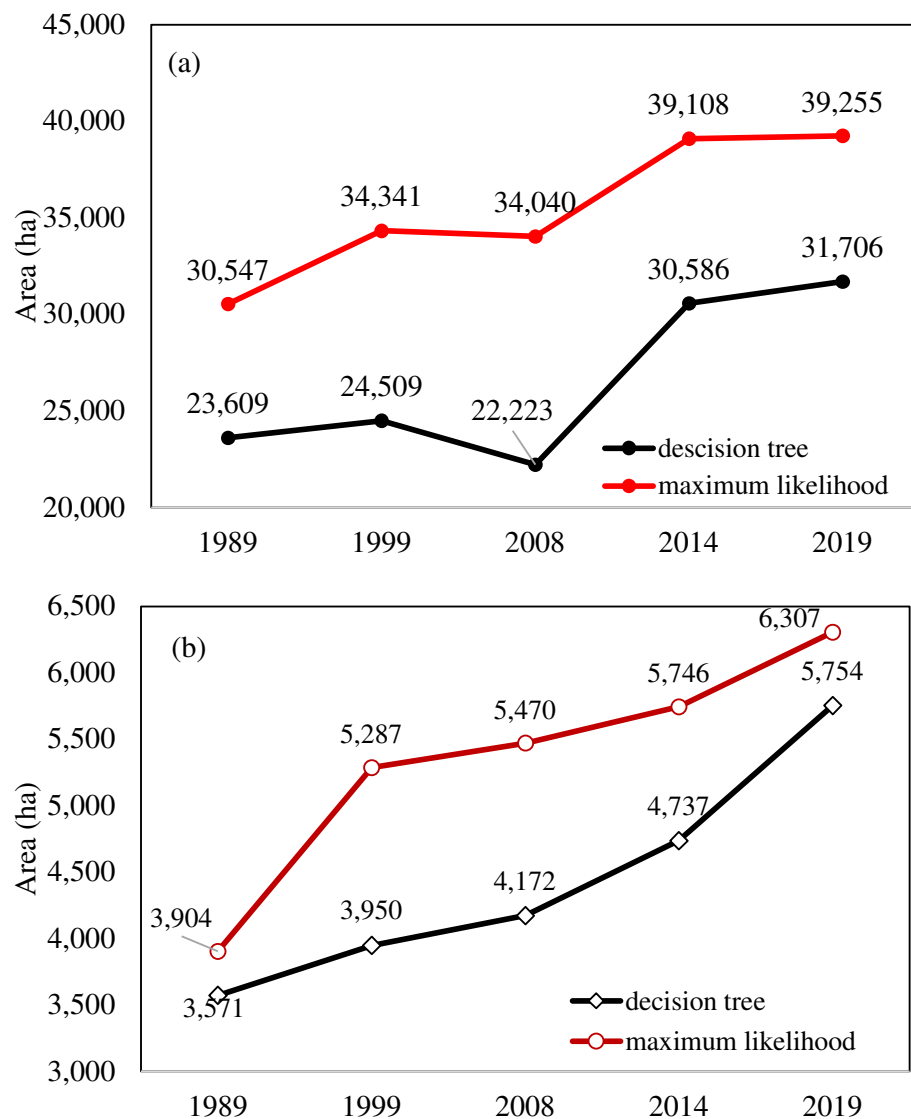
Figure 5. Change in (**a**) cropland and (**b**) orchard area from 1989 to 2019 in the Qom province.

Figure 6 illustrates the trend of cropland area change from 1989 to 2019 separately for spring and fall croplands (regarding the DTC method). As in the MLC method, the samples taken for classification can only be generalized in one image, so it is not possible to separate spring and fall cultivation areas, but the total cropland area can be calculated from an image.

The spring croplands during this period increased from 11,728 ha to 17,323 ha, i.e., a growth of 46%, and fall cropland increased by 21% from 11,880 ha to 14,383 ha. In the case of orchards, DTC demonstrates an increased rate of approximately 60% (2% annually). As can be seen in Figure 5a, the cropland area in 2008 compared to 1999 in both classification methods shows a considerable decrease. However, according to DTC results (Figure 6), it is clear that this reduction area relates to fall cropland, and spring cropland has not reduced significantly.
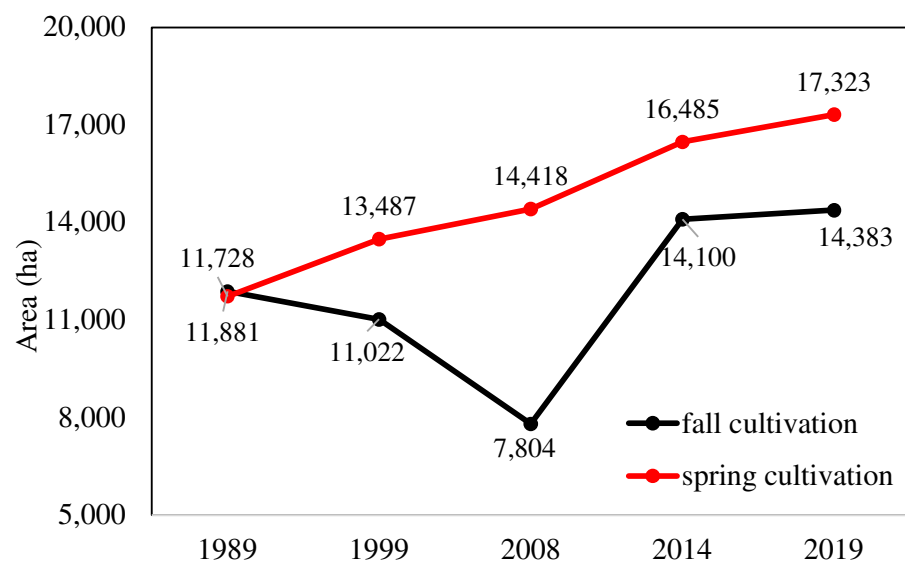
Figure 6. Trend of changes in area in spring and fall cultivation based on DTC.

4.3. Trend of Net Water Consumption

Using Equation (9), the average net water demands of crop and orchard products were calculated as 369.069 and 10,358.16 cubic meters per hectare (m³/ha), respectively. Taking the average net water consumption and the area of croplands and orchards from the previous section, the trend of net water consumption in the agricultural sector of Qom province in the 30-year period can be easily calculated. As shown in Figure 7a, the net water demand for the agricultural class (irrigated agriculture) in the MLC increased from 111 million cubic meters (mcm) to 143 mcm. This shows a growth of 29% in net water consumption. Additionally, the net water demand for the orchard class increased from 40 mcm to 65 mcm (25 mcm enhancement) over the 30-year period, which shows a growth of 62%. The whole net water consumption of the agricultural sector (croplands and orchards) of the province during this 30-year period increased from 152 mcm to 209 mcm, which shows a 38% increase in water consumption (equal to 1.26% annually).

According to DTC results (Figure 7b), the net irrigation requirement for the agricultural sector increased from 86 mcm to 116 mcm at the end of the period. The net irrigation requirement of the orchard increased from 37 mcm to 59 mcm, which shows an increase of 60%. The amount of net water consumed in the agricultural sector of Qom province (spring croplands, fall croplands, and orchard) increased from 123 mcm to 175 mcm in the 30-year period. This increase in water consumption equals a growth of 42% (1.4% enhancement annually). This enhancement of water consumption in a place with limited water resources in an arid area is questionable. This increase in the net water consumption may be the major reason for many problems in Qom province, such as groundwater depletion [34,35], surface water and storage reduction [36], land subsidence [37], saltwater intrusion [38], and water quality degradation [36].
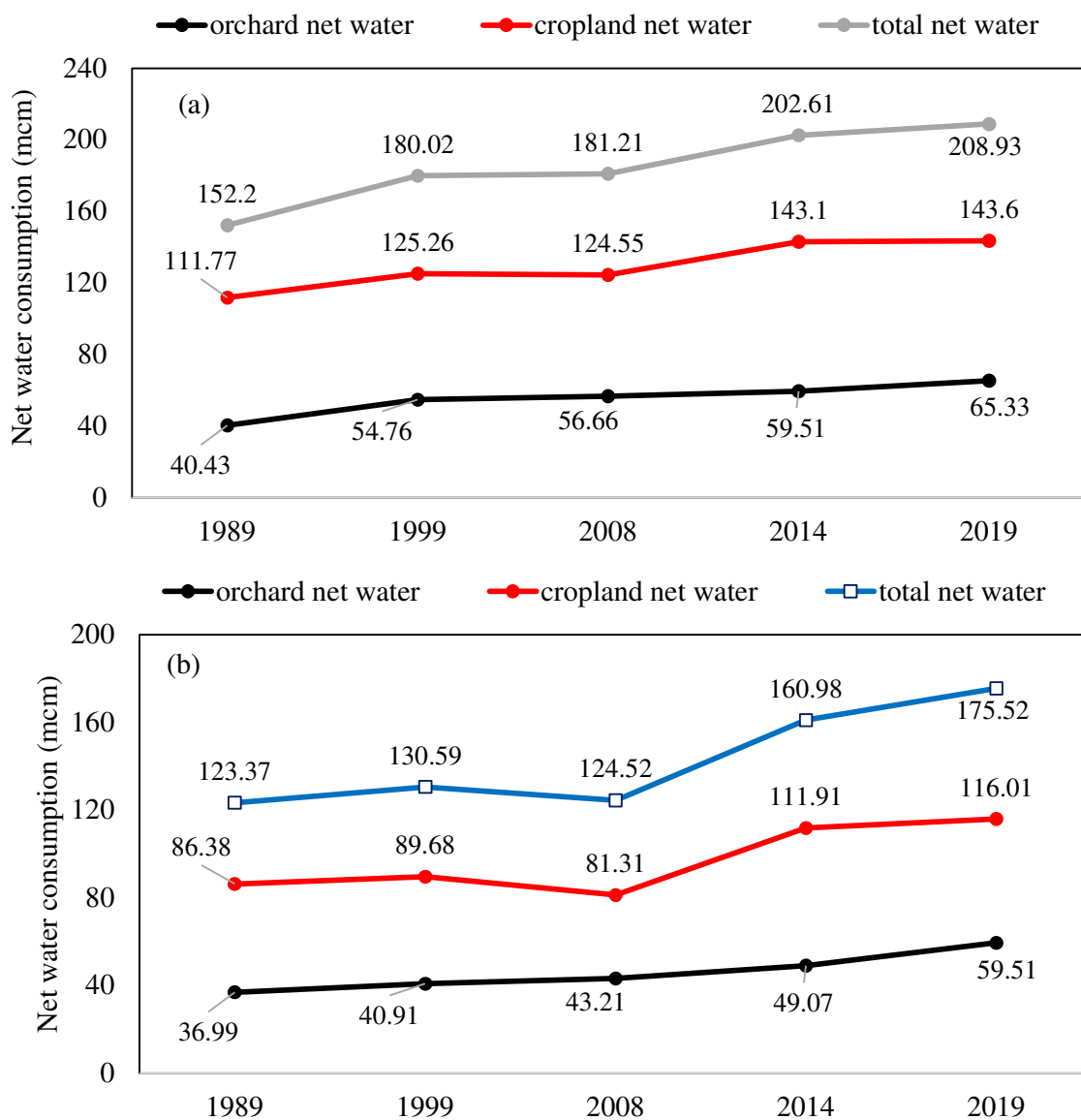
Figure 7. Trend of net water consumption in Qom province agricultural sector by (**a**) MLC and (**b**) DTC.

5. Conclusions

Due to extensive desertification worldwide, the treatment of hyper-arid regions is of particular relevance [39,40]. Qom province is one of the important provinces of Iran according to its climate and socio-economic aspects and one of the top five provinces in terms of high water stress. Therefore, managing water demand is very important, although inter-basin water transfer has also been cited as one of the major strategies to overcome water stress in this province. Because of water importance and the need to establish effective strategies, especially in the arid regions [39,40], to overcome the present and future challenges, this study aimed to evaluate the trend of land-use changes and assess the changes in water demand in Qom province over the past thirty years. To extract the different land uses, a remote sensing technique was employed, and two different methods of MLC and DTC were examined for classification. The results of MLC showed an increase of 57 mcm of agricultural water demand (cropland and orchard) over the 30-year period. According to the results from 1989 to 2019, net irrigation water in the Qom province increased from 152 mcm to 209 mcm. The net irrigation requirement for croplands and orchards increased, respectively, by almost 29% and 62% (overall 38%). This increase in

water demand in the 30-year period is directly related to the increasing trend of croplands and orchards. According to the obtained results, the cropland area increased from 30,546 ha in 1989 to 39,255 ha in 2019, which shows a 29% growth. Regarding the orchard land-use class, a 61% increase was observed (from 3903 ha in 1989 to 6306 ha in 2019). On the other hand, assessment of the results of the DTC method showed an increase of 52 mcm in agricultural water demand (cropland and orchard), so the net water consumption increased from 123 mcm in 1989 to 175 mcm in 2019. Meanwhile, the amount of increasing water demand of cropland classes was 34%, and the amount of increasing water demand of orchard classes was 61%. This increase in water demand from 1989 to 2019 is related to the increasing trend of agricultural land use (spring and fall croplands) and orchard class. Based on the DTC results, agricultural land use (spring and fall croplands) in 1989 increased from 23,608 ha to 31,706 ha in 2019, which shows a 34% increase. Regarding the orchard class, a 60% increase in the cultivation area was observed. In total, the results of both classification methods showed a 38% and 39% increase in the net water demand in this 30-year period. Currently, most of the province's agricultural water demands are supplied from groundwater aquifers. The continuation of this trend due to the limited water resources of the province is a difficult challenge for water resource management in the future. Land-use changes in agricultural practices from rainfed to irrigated or from low to high-water-demand crops in the region have caused such an increase in water consumption in the province. Unfortunately, in recent decades, in addition to the uncontrolled consumption of groundwater resources, several inter-basin water transfer projects were implemented in this province as well. These transfer projects have been implemented to overcome the issue of drinkable water shortage that has been increasing due to population growth. The latest water transfer project is related to the water supply of Qom province from the Kouchari dam in the adjacent province. The transferred water amount has increased from 27 mcm in 2010 to almost 255 mcm in 2020. This increase is in line with the water demand increase in the agricultural sector. In other words, as a result of this increasing trend, these projects have been planned and performed.

Author Contributions: Conceptualization, F.H., S.R.-G. and R.N.; methodology, F.H.; software, A.E.; validation, R.N. and M.M.S.; formal analysis, R.N., S.R. and M.M.S.; data curation, R.N.; writing—original draft preparation, A.E.; writing—review and editing, F.H., S.R.-G., S.R., R.N., M.M.S. and M.K.; visualization, S.R.; supervision, F.H. and R.N. All authors have read and agreed to the published version of the manuscript.

Data Availability Statement: The datasets generated during and/or analyzed during the current study are available from the corresponding author upon reasonable request.

Conflicts of Interest: The authors declare that they have no known competing financial interests or personal relationships that could have appeared to influence the work reported in this paper.

References

1. Teka, H.; Madakadze, C.I.; Botai, J.O.; Hassen, A.; Angassa, A.; Mesfin, Y. Evaluation of Land Use Land Cover Changes Using Remote Sensing Landsat Images and Pastoralists Perceptions on Range Cover Changes in Borana Rangelands, Southern Ethiopia. *Int. J. Biodivers. Conserv.* **2018**, *10*, 1–11. [CrossRef]
2. Hua, A.K. Land Use Land Cover Changes in Detection of Water Quality: A Study Based on Remote Sensing and Multivariate Statistics. *J. Environ. Public Health* **2017**, *2017*, 7515130. [CrossRef] [PubMed]
3. Mahdian, M.; Hosseinzadeh, M.; Siadatmousavi, S.M.; Chalipa, Z.; Delavar, M.; Guo, M.; Abolfathi, S.; Noori, R. Modelling Impacts of Climate Change and Anthropogenic Activities on Inflows and Sediment Loads of Wetlands: Case Study of the Anzali Wetland. *Sci. Rep.* **2023**, *13*, 5399. [CrossRef]
4. Zhou, Q.; Li, B.; Sun, B. Modelling Spatio-Temporal Pattern of Landuse Change Using Multi-Temporal Remotely Sensed Imagery. *Int. Arch. Photogramm. Remote Sens. Spat. Inf. Sci.* **2008**, *37*, 729–734.
5. Singh, R.L.; Singh, P.K. Global environmental problems. In *Principles and Applications of Environmental Biotechnology for a Sustainable Future*; Springer: Singapore, 2017; pp. 13–41.

6.	Modabberi, A.; Noori, R.; Madani, K.; Ehsani, A.H.; Mehr, A.D.; Hooshyaripor, F.; Kløve, B. Caspian Sea Is Eutrophying: The Alarming Message of Satellite Data. *Environ. Res. Lett.* **2020**, *15*, 124047. [CrossRef]

7.	Mozafari, Z.; Noori, R.; Siadatmousavi, S.M.; Afzalimehr, H.; Azizpour, J. Satellite-Based Monitoring of Eutrophication in the Earth's Largest Transboundary Lake. *GeoHealth* **2023**, *7*, e2022GH000770. [CrossRef]

8.	Hussain, S.; Mubeen, M.; Karuppannan, S. Land Use and Land Cover (LULC) Change Analysis Using TM, ETM+ and OLI Landsat Images in District of Okara, Punjab, Pakistan. *Phys. Chem. Earth Parts a/b/c* **2022**, *126*, 103117. [CrossRef]

9.	Lagrosa, J.J., IV; Zipperer, W.C.; Andreu, M.G. An Ecosystem Services-Centric Land Use and Land Cover Classification for a Subbasin of the Tampa Bay Watershed. *Forests* **2022**, *13*, 745. [CrossRef]

10.	Zarandian, A.; Ramezani Mehrian, M.; Mohammadyari, F. Impact Assessment of Vegetation Loss on the Ecosystem Functions in a Semiarid Watershed in Iran. *Acta Geophys.* **2022**, *70*, 677–696. [CrossRef]

11.	Liang, F.; Zhang, X.; Li, H.; Yu, H.; Lin, Q.; Jiang, M.; Zhang, J. Land Use Classification Based on Maximum Likelihood Method. In *Advances in Intelligent Data Analysis and Applications, Proceedings of the Sixth Euro-China Conference on Intelligent Data Analysis and Applications, Arad, Romania, 15–18 October 2019*; Springer: Singapore, 2022; pp. 133–139.

12.	Saraf, S.; Vejahat, J. Assessment of quantitative and qualitative characteristics of rivers in the catchment area of the Salt Lake in Alborz Province of Iran. *Cent. Asian J. Environ. Sci. Technol. Innov.* **2022**, *3*, 128–142.

13.	Chughtai, A.H.; Abbasi, H.; Karas, I.R. A Review on Change Detection Method and Accuracy Assessment for Land Use Land Cover. *Remote Sens. Appl. Soc. Environ.* **2021**, *22*, 100482. [CrossRef]

14.	Rohani, N.; Rajaee, T.; Mojaradi, B.; Jabbari, E.; Shafiei Darabi, S.A.; Heidari Bani, M. Climate Study of Changes of Major Water Resources in Qom Province Using Satellite Data and Remote Sensing Technologies. *Environ. Sci.* **2021**, *19*, 239–258.

15.	Verma, P.; Singh, P.; Srivastava, S.K. Impact of Land Use Change Dynamics on Sustainability of Groundwater Resources Using Earth Observation Data. *Environ. Dev. Sustain.* **2020**, *22*, 5185–5198. [CrossRef]

16.	Hu, Y.; Batunacun; Zhen, L.; Zhuang, D. Assessment of Land-Use and Land-Cover Change in Guangxi, China. *Sci. Rep.* **2019**, *9*, 2189. [CrossRef] [PubMed]

17.	Nodefarahani, M.; Aradpour, S.; Noori, R.; Tang, Q.; Partani, S.; Kløve, B. Metal Pollution Assessment in Surface Sediments of Namak Lake, Iran. *Environ. Sci. Pollut. Res.* **2020**, *27*, 45639–45649. [CrossRef]

18.	Mosammam, H.M.; Nia, J.T.; Khani, H.; Teymouri, A.; Kazemi, M. Monitoring Land Use Change and Measuring Urban Sprawl Based on Its Spatial Forms: The Case of Qom City. *Egypt. J. Remote Sens. Space Sci.* **2017**, *20*, 103–116.

19.	Nemati, A.; Ghoreishi Najafabadi, S.H.; Joodaki, G.; Mousavi Nadoushni, S.S. Evaluation of Agricultural Drought Characteristics in Iran's Central Plateau Catchment Using GRACE Satellite. *Iran. J. Soil Water Res.* **2019**, *50*, 313–327.

20.	Noori, R.; Maghrebi, M.; Jessen, S.; Bateni, S.M.; Heggy, E.; Javadi, S.; Nouri, M.; Pistre, S.; Abolfathi, S.; AghaKouchak, A. Decline in Iran's Groundwater Recharge. *Nat. Commun.* **2023**, *14*, 6674. [CrossRef]

21.	Pakseresht, S. *Strategic Problemology of Development in Qom Province*; Center for Presidential Strategic Studies: Tehran, Iran, 2016.

22.	Karimi, N.; Bagheri, M.H.; Hooshyaripor, F.; Farokhnia, A.; Sheshangosht, S. Deriving and evaluating bathymetry maps and stage curves for shallow lakes using remote sensing data. *Water Resour. Manag.* **2016**, *30*, 5003–5020. [CrossRef]

23.	Zha, Y.; Gao, J.; Ni, S. Use of normalized difference built-up index in automatically mapping urban areas from TM imagery. *Int. J. Remote Sens.* **2003**, *24*, 583–594. [CrossRef]

24.	Ahmad, A.; Quegan, S. Analysis of maximum likelihood classification on multispectral data. *Appl. Math. Sci.* **2012**, *6*, 6425–6436.

25.	Friedl, M.A.; Brodley, C.E. Decision tree classification of land cover from remotely sensed data. *Remote Sens. Environ.* **1997**, *61*, 399–409. [CrossRef]

26.	Dittrich, A.; Buerkert, A.; Brinkmann, K. Assessment of Land Use and Land Cover Changes during the Last 50 Years in Oases and Surrounding Rangelands of Xinjiang, NW China. *J. Agric. Rural Dev. Trop. Subtrop.* **2010**, *111*, 129–142.

27.	Ebadzadeh, H.; Ahmadi, K.; Mohammadnia-Afrozi, S.; Abbastaghani, R.; Moradi-Islami, A.; Abbasi, M.; Yari, S. *Agricultural Statistics*; Agricultural-Jihad Organization of Qom Province: Qom, Iran, 2014.

28.	Banko, G. *A Review of Assessing the Accuracy of Classifications of Remotely Sensed Data and of Methods Including Remote Sensing Data in Forest Inventory*; International Institute for Applied Systems Analysis: Luxemburg, 1998.

29.	Sharma, S.; Pradhan, R. Classification Methods for Land Use and Land Cover Pattern Analysis. *Int. J. Innov. Technol. Explor. Eng.* **2014**, *4*, 36–38.

30.	Alizadeh, A.; Kamali, G. *Crops Water Requirement in Iran*; Imam Reza University: Mashhad, Iran, 2008.

31.	Preite, L.; Solari, F.; Vignali, G. Technologies to Optimize the Water Consumption in Agriculture: A Systematic Review. *Sustainability* **2023**, *15*, 5975. [CrossRef]

32.	Rosenfield, G.H.; Fitzpatrick-Lins, K. A Coefficient of Agreement as a Measure of Thematic Classification Accuracy. *Photogramm. Eng. Remote Sens.* **1986**, *52*, 223–227.

33.	Cohen, J. A Coefficient of Agreement for Nominal Scales. *Educ. Psychol. Meas.* **1960**, *20*, 37–46. [CrossRef]

34.	Noori, R.; Hooshyaripor, F.; Javadi, S.; Dodangeh, M.; Tian, F.; Adamowski, J.F.; Berndtsson, R.; Baghvand, A.; Klöve, B. PODMT3DMS-Tool: Proper orthogonal decomposition linked to the MT3DMS model for nitrate simulation in aquifers. *Hydrogeol. J.* **2020**, *28*, 1125–1142. [CrossRef]

35.	Maghrebi, M.; Noori, R.; Partani, S.; Araghi, A.; Barati, R.; Farnoush, H.; Torabi Haghighi, A. Iran's Groundwater Hydrochemistry. *Earth Space Sci.* **2021**, *8*, e2021EA001793. [CrossRef]

36. Yaghmaei, H.; Sadeghi, S.H.; Moradi, H.; Gholamalifard, M. Effect of Dam Operation on Monthly and Annual Trends of Flow Discharge in the Qom Rood Watershed, Iran. *J. Hydrol.* **2018**, *557*, 254–264. [CrossRef]
37. Rajabi, A.M. A Numerical Study on Land Subsidence Due to Extensive Overexploitation of Groundwater in Aliabad Plain, Qom-Iran. *Nat. Hazards* **2018**, *93*, 1085–1103. [CrossRef]
38. Noori, R.; Maghrebi, M.; Mirchi, A.; Tang, Q.; Bhattarai, R.; Sadegh, M.; Noury, M.; Torabi Haghighi, A.; Kløve, B.; Madani, K. Anthropogenic Depletion of Iran's Aquifers. *Proc. Natl. Acad. Sci. USA* **2021**, *118*, e2024221118. [CrossRef] [PubMed]
39. Foldvary, L.; Abdelmohsen, K.; Ambrus, B. Water Density Variations of the Aral Sea from GRACE and GRACE-FO Monthly Solutions. *Water* **2023**, *15*, 1725. [CrossRef]
40. Xu, L.; Chen, N.C.; Zhang, X. Global drought trends under 1.5 and 2 °C warming. *Int. J. Climatol.* **2019**, *39*, 2375–2385. [CrossRef]